Int. J. Heat Mass Transfer. Vol. 8, pp. 793–814. Pergamon Press 1965. Printed in Great Britain

BURNOUT AND NUCLEATION IN CLIMBING FILM FLOW

G. F. HEWITT, H. A. KEARSEY, P. M. C. LACEY* and D. J. PULLING
Atomic Energy Research Establishment, Harwell, Berkshire

(*Received* 4 *January* 1964 *and in revised form* 9 *November* 1964)

Abstract—Studies have been made of the behaviour of a water film on the heated central rod of an annular test section carrying flowing steam at atmospheric pressure, the water having been introduced through a porous wall. The outer glass wall of the annulus was heated to prevent condensation and droplet deposition, and hence the inner rod surface was rendered clearly visible. The onset of nucleation within the film was demonstrated and the conditions for its initiation were determined and compared with theoretical predictions; in other experiments "burnout", or "dry-out", heat flux measurements were made and related to the measured residual film flow on the heated rod. Visual and photographic studies revealed a relatively stable condition of break-up of the climbing film, with rivulets around dried-out patches, before the burnout trip operated.

The residual film flow rate at which dry patches appeared was very small indeed and the "burnout" phenomenon was clearly the result simply of total loss of water from the film by evaporation and entrainment; the local value of the heat flux at the site of the burnout was evidently of only secondary relevance. There was evidence that bubble nucleation in the film could contribute appreciably to the loss by entrainment at high heat fluxes.

1. INTRODUCTION

FOR A NUMBER of years now the phenomenon of "critical heat flux" or "burnout" has been the object of intensive study. A great quantity of data has been obtained for a wide variety of test sections and for pressures up to critical and above. More recently the field has been extended to organic, cryogenic and liquid metal systems. Although much excellent work has been done, knowledge of the precise nature of burnout and of the closely interrelated phenomenon of steam bubble nucleation is still incomplete. This latter fact is mainly due to the very complex nature of the flow of two-phase mixtures and also to the difficulty of seeing and photographing the processes of burnout and nucleation in forced convective systems.

The present paper describes the first results† from an experiment in which burnout and nucleation in the climbing film regime of flow could be directly observed and in which a new type of measurement could be made, viz. that of the rate of flow of the water film at the exit end of the heater.

The experiment has been carried out at low pressure and the test section is an annulus. It is arranged that only the inner, heated, surface is wetted; the outer surface, of glass, is kept substantially dry, by external heating, and the central heater rod surface can be viewed through it. This is achieved by passing dry steam in at the bottom of the annulus and introducing the liquid film on to the central rod through a porous sinter. The flow rate in the liquid film becomes depleted due to nucleate boiling and/or surface evaporation and entrainment and its value at the end of the heat section is determined by sucking the film off through a further sinter; this latter measurement is essential to an understanding of the behaviour of the system.

2. EXPERIMENTAL

2.1 *Apparatus*

A flow diagram of the apparatus is shown in Fig. 1. Steam from the 100 psi main, was reduced in pressure to about 40 psi and passed through a cyclone, a drier and an electrically heated pipe superheater. After receiving a few degrees of superheat the steam passed through an orifice plate coupled to a differential pressure cell and then via the steam flow control valve to the test section. The orifice plate calibration was checked before each experiment by weighing the condensate flow.

* Present Address: Department of Chemical Engineering, University of Exeter.

† Confirmed in subsequent investigations.

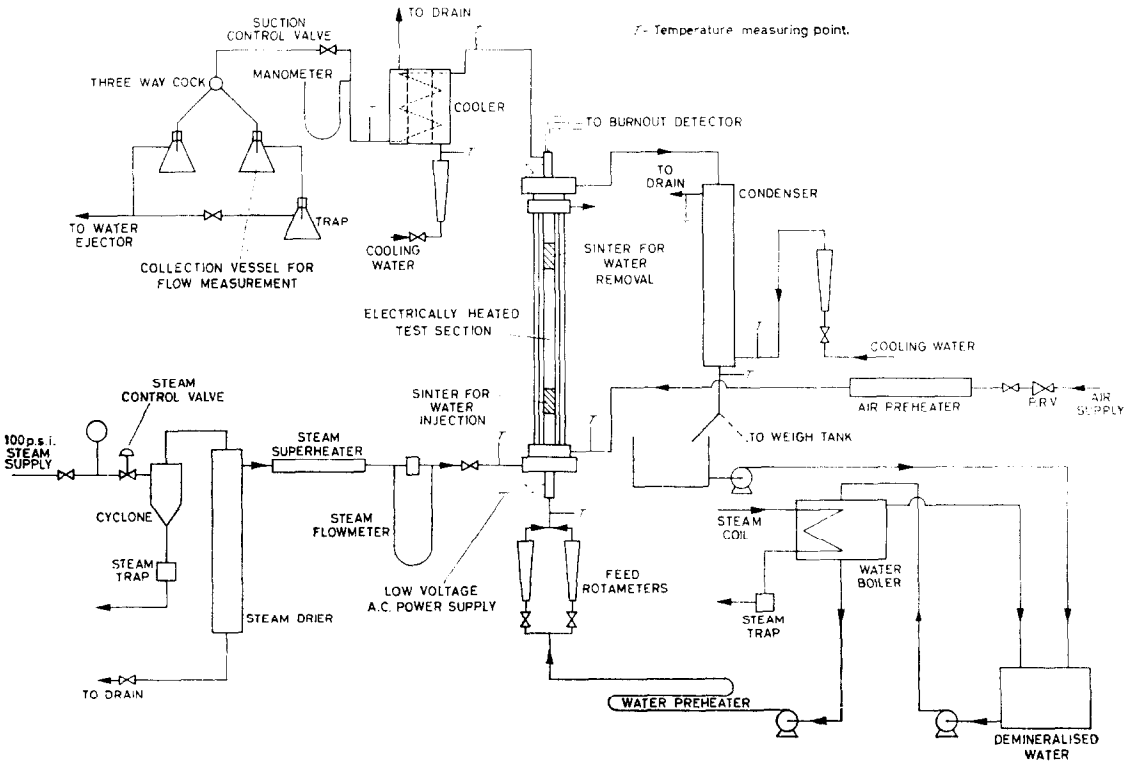

FIG. 1. Flow diagram of apparatus.

Water from a boiler tank was fed to the test section by a Mono pump via calibrated Rotameters and an electrically heated pipe preheater.

The core rod of the test section is shown in detail in Fig. 2. It consisted of a 0·5 in diameter rod and was mounted centrally inside a precision bore glass tube 0·866 in i.d. One portion of the rod was made from 24 swg stainless steel tubing, and heat was generated in it by passing a low-voltage alternating current; the effective heated length was 14·5 in. The remainder of the rod was made from copper and extended through glands in the headers to enable electrical connections to be made.

The water was introduced as a film on the rod by feeding it up the centre of the lower copper conductor and out through a porous bronze sinter. The sinter was mounted 6 in below the heated section to allow a hydrodynamic calming length.

A second bronze sinter (0·5 in long) was mounted at the top of the heated section. By means of this sinter, water flowing on the rod could be sucked off and passed through a cooler to allow the film flow to be measured; the suction was applied by means of a water ejector.

The steam entered through the bottom header and flowed in the annulus between the rod and the glass flowtube. Owing to the design of the header and the hollow rod, the steam lost almost all its superheat to the surroundings and to the water; this meant that at the point where the water left the sinter, both it and the steam were very close to saturation temperature.

The flowtube was surrounded by a second glass tube, and hot air (approximately 230°C) was passed through the annulus between them, to prevent condensation on the inner surface of the flowtube.

In order to protect the heater from physical

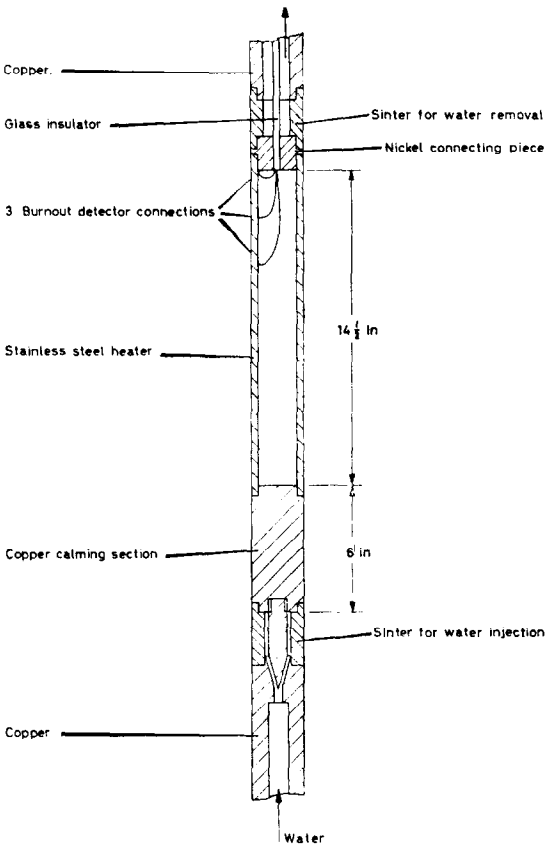

FIG. 2. Test section core rod. (Mounted concentric with 0·866 in i.d. glass flow tube.)

burnout, a trip was fitted. Three electrical connections were made to the inside of the heater tube at the exit end, 3 in apart, and brought up the inside of the upper copper conductor. The two sections of the heater were used as arms of a bridge circuit, and the unbalance due to temperature excursions when burnout was imminent was used to operate a high speed electrical circuit breaker in the heater circuit [1].

The steam and water mixture leaving the test section passed to a water-cooled condenser. The temperature and flow rate of both the condensate and the cooling water could be measured to enable a heat balance to be carried out. The mixture of steam and water which was sucked off through the upper sinter was passed through a cooler and the two phases differentiated by making calorimetric measurements. The cooler consisted of a coiled pipe in an annular bath of cooling water. The cooler and the pipe connecting it to the test section were carefully lagged and the inlet temperature of the steam–water mixture was taken as the saturation temperature measured at the top of the test section. The suction pressure at the outlet to the cooler was measured on a water-over-mercury manometer, and was adjusted by means of a control valve after the cooler. The condensate flow rate was measured by diverting the flow into a separate vessel connected to the same vacuum supply.

2.2 *Experimental procedure for obtaining quantitative data*

The steam and water flows were first adjusted to their required values. To carry out a determination of burnout heat flux, the power applied to the heater was gradually raised, the flows being kept constant. At the first visible sign of a breakdown of the liquid film, the power applied was noted. This will be referred to as the point of film breakdown. The power was then raised further until the burnout trip operated, and this will be referred to as the burnout point.

In order to observe the onset of nucleation, the flows were set as before and the power raised slowly. The heated section was closely observed for the first appearance of a nucleation point, its location and the power being noted. The power was then raised again, but only the section of the heater above the previous nucleation point was scrutinized for the next nucleation point. The process was continued until the burnout point was reached.

Whilst a film flow rate measurement was being carried out, the condensate from the main condenser was collected and weighed at the same time as that from the film flow rate measurement cooler, in order to provide a mass balance.

It was usually possible to combine all these measurements within each run.

3. RESULTS

3.1 *Qualitative observations*

One of the main advantages in using the test section design illustrated in Fig. 2, is that the phenomena which are occurring on the heated rod can be observed directly and clearly. Full

advantage was taken of this facility both by direct visual observation and by high-speed ciné-photography. The observations can best be summarized by considering the behaviour of the film on the heated rod as the heat flux was increased from zero to the burnout value.

At zero heat flux, the film flowed along the rod without much visible change in nature after the first few inches. As the liquid rate was increased or the gas rate decreased the liquid film became more and more wavy. These surface waves gave rise to entrainment, some of which was transferred to the outer wall of the annulus; sometimes a thin film of liquid was formed on this outer wall since heat was not transferred through the wall at sufficient rate to cause more than a minimal amount of evaporation. This thin film on the outer wall did not interfere seriously with the view of the inner rod.

When a heat flux was applied, water was lost from the film by direct evaporation from the liquid surface or by generation of steam bubbles on the heated rod (i.e. by nucleation). The reduction of the water flow rate in the film led to the attenuation of the large disturbance waves on the film surface and eventually, at a point near the top of the heater, a small dry patch began to appear intermittently. This dry patch began to grow down the rod and others appeared around it as the heat flux was further increased. The liquid flowed in narrow streams around the dry patches which now had a continuous existence, although their boundaries were oscillating. The areas of the surface which were dry were, of course, still being heated and the rod rose in temperature at these points; eventually this rise in temperature was sufficient to cause the resistance-operated trip to come into action.

Whether or not bubble nucleation occurred before the film breakdown point depended upon the flow rates being used; at high steam velocities, no nucleation was observed. When nucleation did occur, it was first seen near the bottom of the rod and as the heat flux was increased, new sites further and further up the rod became active and increased nucleation activity occurred lower down. An interesting phenomenon accompanying nucleation was the ejection of droplets from the film simultaneously with the release of the steam bubble. This effect could be clearly observed in the high-speed ciné films; in many cases, however, the number of active sites was insufficient to make much contribution to the total entrainment. At the point of film breakdown, the liquid tended to form rivulets (as described above) and nucleation was sometimes observed in these rivulets.

3.2 *Quantitative experiments*

Initially, experiments were carried out to determine the burnout heat flux at various combinations of water and steam flows. These

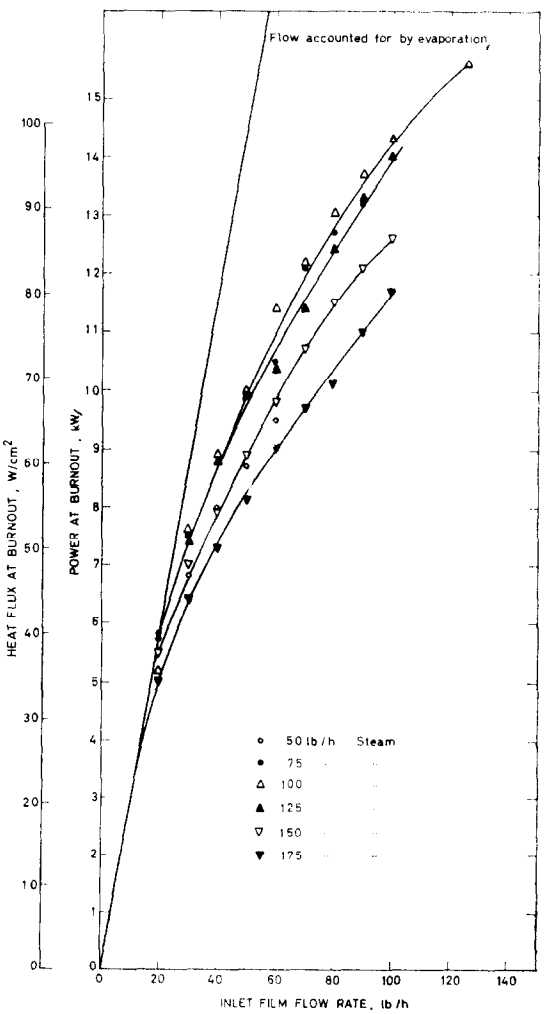

FIG. 3. Burnout heat flux as a function of inlet film flow rate at a series of constant steam rates.

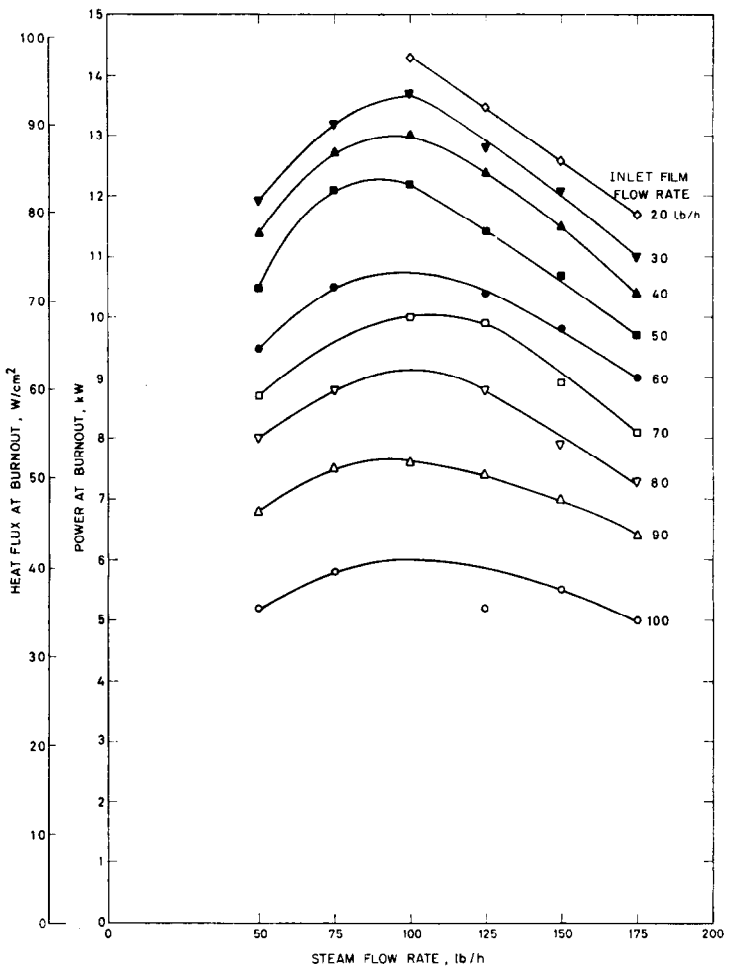

FIG. 4. Burnout heat flux as a function of steam flow at a series of inlet film flow rates.

results are presented in Figs. 3 and 4. The curves at constant inlet steam flow rate (Fig. 3) have a fairly uniform shape; they join the "total liquid evaporation" line at low liquid flow rate, and negative deviation from this line increases with water flow rate. Figure 3 shows that this deviation is least at about 100 lb/h steam flow. Later, all measurements were carried out with steam and water flow rates that gave three fixed total mass flow rates, 4·6, 6·4 and 8·3 $\times$ 10^4 lb/ft^{2}h. Figures 5(a) and 5(b) show the burnout heat flux and film breakdown flux respectively at these mass flow rates, plotted on an exit steam quality basis. The results are tabulated in Table 1. It will be noted that the qualities concerned are relatively high.

The curves drawn through burnout and film breakdown data at constant mass flow rate [in Figs. 5(a) and 5(b)] have been re-drawn for comparison in Fig. 5(c). As one might expect, the burnout curves—which represent the attainment by the rod of an arbitarily determined temperature—are somewhat above the film breakdown curves. The curves are nearly parallel, however, and it is clear that the burnout occurs *because* the film has broken down. The curves for both film breakdown and burnout are relatively flat at the lower qualities, and become steeper as the quality

Table 1. Film breakdown and burnout results

Mass flow rate	Inlet flow		Film breakdown		Burnout	
(lb ft^{-2}h^{-1} × 10^4)	Steam (lb h^{-1})	Water (lb h^{-1})	Power (kW)	Quality (%)	Power (kW)	Quality (%)
4·6	50	75·5	9·9	67·6	11·0	70·7
	50	75·0	9·9	67·9	11·0	70·9
	82·5	42·9	9·3	91·9	9·8	93·3
	75·5	49·9	9·5	86·1	10·2	88·8
	65·6	60·1	10·3	81·0	10·9	82·7
	75·2	50·2	9·3	86·07	10·2	88·6
	100	25	5·5	95·5	6·6	98·6
6·4	49·6	124·1	13·5	55·9	14·2	57·3
	75·2	100·3	13·0	68·9	13·9	70·7
	90·5	85·5			13·7	79·0
	82·8	92·2	13·8	69·4	14·0	75·5
	100·6	75·5	11·3	79·7	12·5	82·1
	124·6	50·1	9	89·4	9·9	91·2
	150·4	24·8	5·3	96·9	6·2	98·7
8·3	78	147	15·4	58·8	16·3	60·2
	75·2	148·5	15·4	57·8	16·1	58·9
	73·6	150·8	15·8	57·8	16·4	58·5
	75·2	150·1	15·8	53·6	16·4	59·0
	82·5	144·2	15·7	60·7	16·3	61·2
	99·8	125·4	14·5	66·98	15·8	69·0
	99·8	125·4	14·6	67·1	15·7	68·8
	100·3	125·4	14·6	67·2	15·4	68·5
	125·4	100·6	12·4	75·0	13·5	76·7
	150	75	10·2	82·6	11·7	85·0
	150	75	10·3	82·8	11·6	84·8
	175	50	7·6	89·7	8·4	90·9
	199·3	25	6·6	98·9	7·6	100·0

increases. It is interesting to note that the lines cross over, leading to a reversal of the effect of mass velocity on going from high to low quality. This is, of course, in agreement with the trends observed by most workers [2]. There are exceptions to this general pattern as the quality approaches 100 per cent.

The data for the onset of nucleation are given in Table 2 and Fig. 6. The heat flux required to start a particular nucleation centre is somewhat un-reproducible. The results for each mass flow rate fall broadly in a band with small positive slope. For comparison purposes, roughly representative bands have been drawn on the graphs. Conditions at a point on the heater which falls within a band will not necessarily give rise to a nucleating site, owing to the wide variation in size of sites on practical surfaces.

The nucleation bands are compared with the film breakdown curves in Fig. 7.

The flow rate in the water film at the end of the heater was determined by sucking it off at that point, but the measured value had to be corrected to allow for any steam withdrawn simultaneously. This was done by carrying out a heat balance over the cooler using the following equation:

$$(W_w + W_s)(T_{sat} - T_3) + \lambda W_s = W_c(T_1 - T_2) \quad (1)$$

where W_s and W_w are the weight flow rates of steam and water respectively, W_c is the weight flow rate of cooling water, T_1 and T_2 are the outlet and inlet temperature of the cooling water, λ is the latent heat, T_3 is condensate outlet temperature and T_{sat} the saturation temperature at the top of the test section.

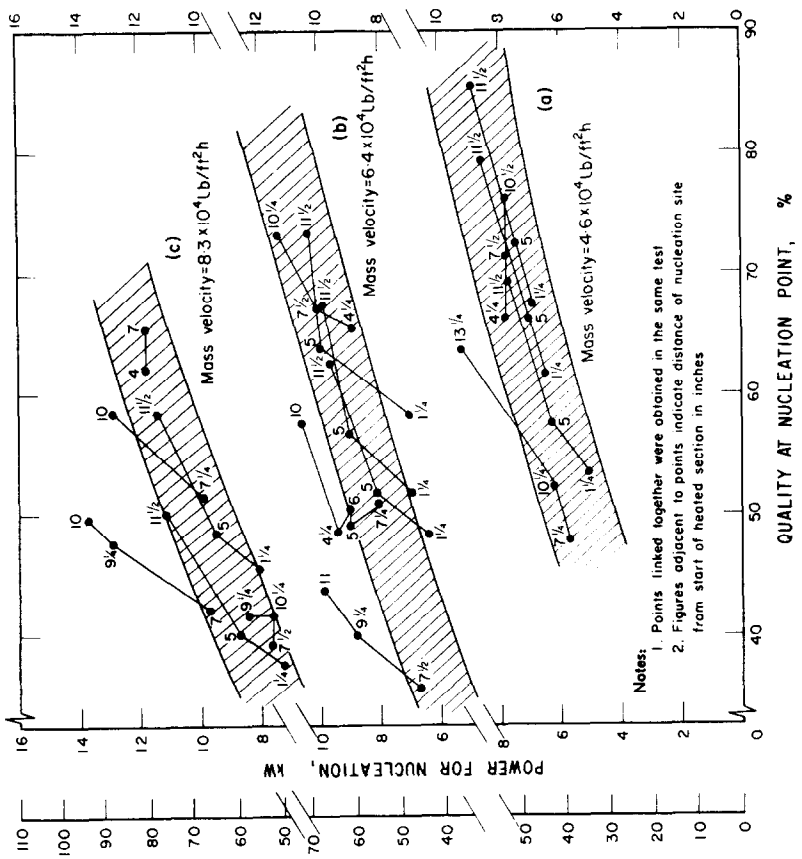

FIG. 6(a, b, c). Heat flux for nucleation.

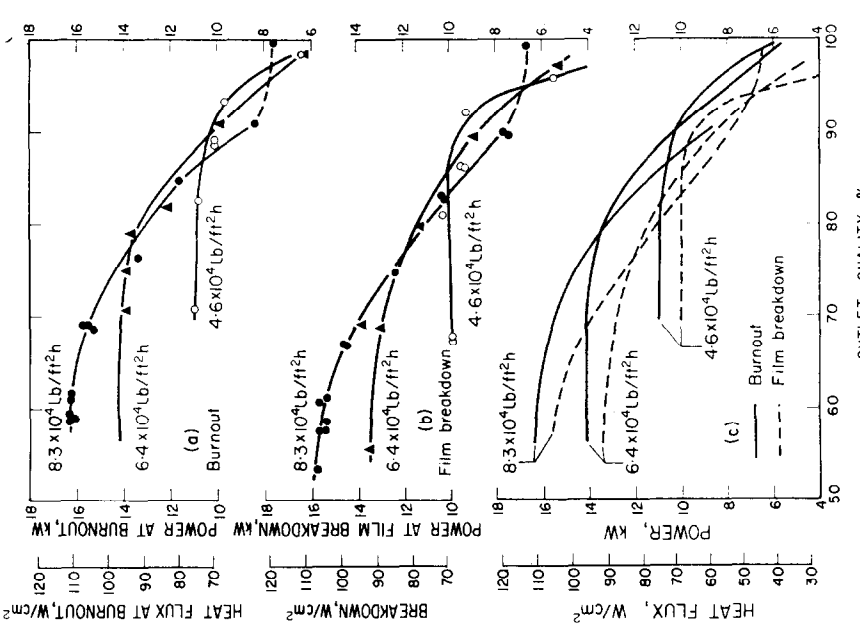

FIG. 5. (a) Burnout at constant mass velocity; (b) onset of film breakdown at constant mass velocity; (c) comparison of film breakdown and burnout curves at constant mass velocities.

Table 2. Initiation of nucleate boiling

Mass flow rate (lb ft^{-2}h^{-1} × 10^4)	Inlet Flow		1st Nucleation Point			2nd Nucleation Point			3rd Nucleation Point		
	Steam (lb/h)	Water (lb/h)	Power (kW)	Distance from inlet (in)	Quality (%)	Power (kW)	Distance from inlet (in)	Quality (%)	Power (kW)	Distance from inlet (in)	Quality (%)
4·6	82·5	42·9	6·9	1¼	67·6	7·5	5	72·3	8·9	11½	85·5
	75·5	49·9	6·5	1¼	61·7	7·0	5	66·2	8·6	11½	79·3
	65·6	60·1	5	1¼	53·3	6·3	5	57·7	7·7	11½	69·2
	75·2	50·2	7·8	4¼	66·3	7·8	7½	71·3	7·8	10½	75·8
	50·0	75·5	5·7	7¼	47·8	6·2	10¼	52·2	9·3	13¼	63·7
6·4	100	75·5	7	1¼	58·2	9·9	5	63·8	10·3	11½	73·4
	90·5	85·5	6·9	1¼	51·8	9·0	5	56·8	9·9	11½	67·1
	82·8	92·2	6·4	1¼	48·3	8·1	5	51·7	9·6	11½	62·6
	100·6	75·5	8·9	4¼	65·4	10·0	7¼	67·1	11·3	10¼	73·1
	75·2	100·7	8	7¼	50·9	9	5	49·1	9	6	50·3
	75·2	100·7	9·4	4¼	48·4	10·6	10	57·5			
	49·6	124·1	6·7	7½	35·6	8·8	9¼	39·9	9·8	11	43·6
8·3	82·8	144·2	7·2	1¼	37·4	8·7	5	40·1	11·1	11½	50·0
	100·0	126·0	8·0	1¼	45·3	9·5	5	48·3	11·4	11½	58·3
	125·4	100	11·8	4	62·0	11·8	7	65·4			
	100·3	125·4	9·9	7¼	51·4	12·9	10	58·3			
	74·6	150	7·6	7½	38·9	7·6	10¼	41·6	8·4	9¼	41·6
	78·2	146·8	9·7	7	42·1	12·9	9¼	47·6	13·7	10	49·5

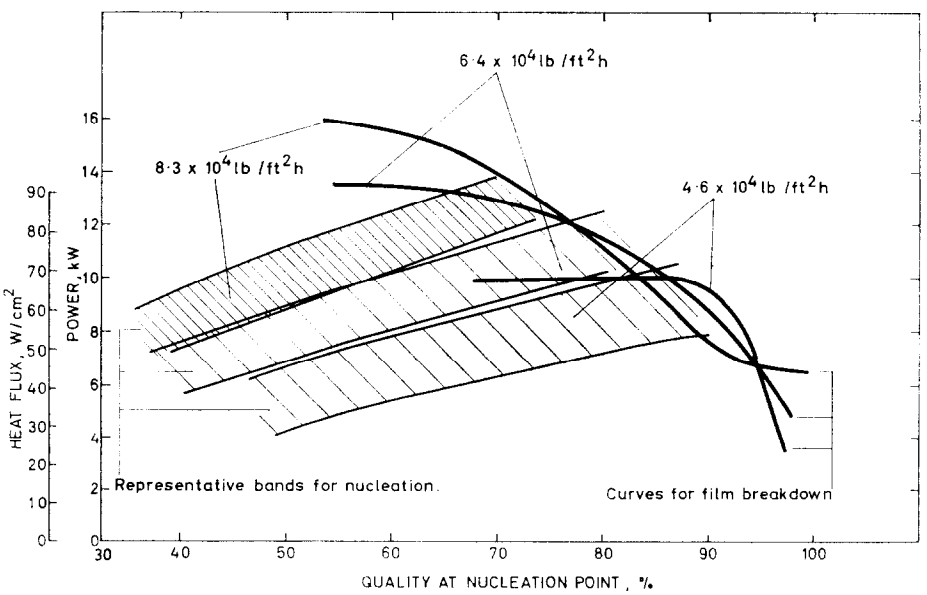

FIG. 7. Comparison of nucleation bands and film breakdown curves.

In order to ensure that the liquid film was being completely removed at the upper sinter, a number of experiments were carried out at several different values of suction pressure; these results are given in Fig. 8. It can be seen that the calculated amount of water sucked off does not alter appreciably with suction pressure over a considerable range. The apparatus was always operated in this range.

At the mass flow rates chosen, the exit film flow rate was measured at selected inlet conditions as a function of heat flux. The results are shown in Figs. 9–12. As one might expect, the exit film flow rate falls continuously with increasing heater power. At zero power, the only mechanism for transferring material out of the liquid film is entrainment; in Fig. 12 the amount removed by entrainment under zero heat flux is plotted against steam quality, and it will be seen that the entrainment flow increases with increasing total flow, but falls with increasing quality. In Figs. 9–11 lines have been added which represent the value of the exit film flow rate at zero power minus the amount evaporated by the input power. The significance of these lines and of their positions relative to the actual film flow rate observations will emerge in later discussions.

It will be noted that the "burnout" occurs very close indeed to the point at which the extrapolated curve of film flow rate versus power cuts the x axis; i.e. at zero flow in the liquid film. The film breakdown occurs at a finite film flow rate but, as can be seen, this flow is only at minor fraction of the total flow evaporated. Film flow rate at breakdown is plotted as a function of exit steam flow rate (i.e. including steam generated in the test section) in Fig. 13. To aid the discussion below, a distinction is drawn between those points at which nucleation was possible before film breakdown and those where it was not. This has been done by considering the "points" in Fig. 7 where the nucleation "bands" intersect their corresponding film breakdown curves.

4. DISCUSSION OF RESULTS FROM PRESENT EXPERIMENTS

In previous papers [3, 4] the theoretical aspects of bubble nucleation and film breakdown have

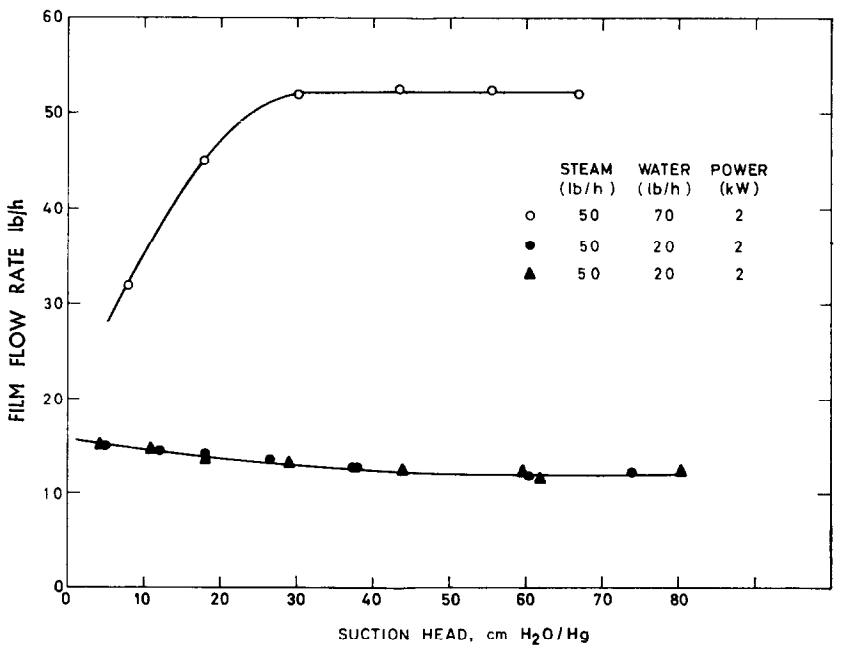

FIG. 8. Effect of suction pressure on film flow rate.

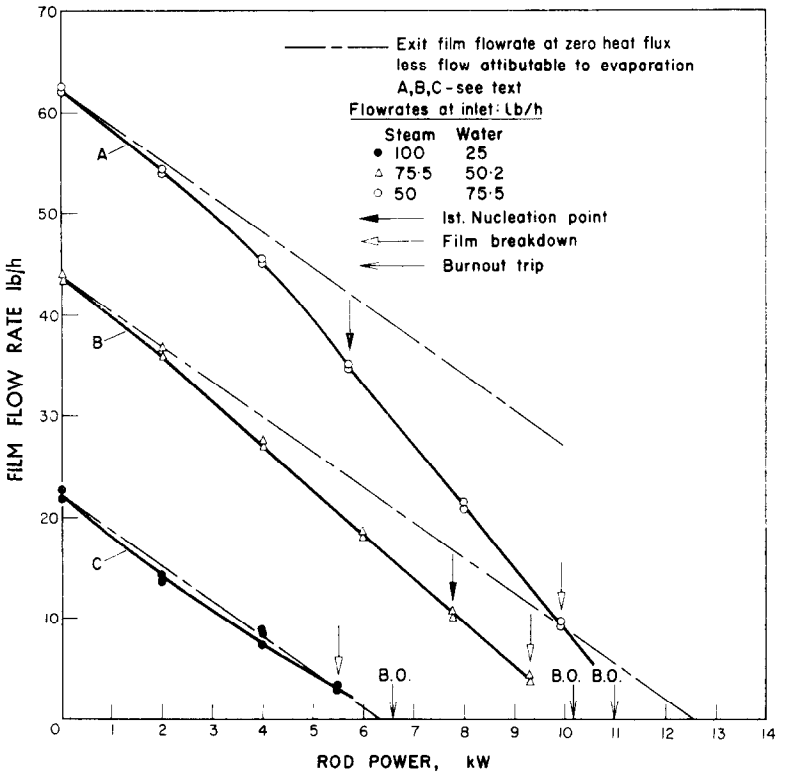

FIG. 9. Effect of power on the film flow rate at the end of the heated section. (Mass flow rate = 4·6 × 10^4 lb/ft^{2}h)

been discussed. In order to make a quantitative comparison between the present data and these theoretical treatments it is necessary to know the shear force at the wetted surface. By making a suitable transformation, [5, 4] it is possible to calculate this shear from a measured value of pressure gradient. Unfortunately, pressure gradients could not be determined in the preliminary experiments reported here. An alternative approach might have been to use a correlation developed previously [6], which relates the film roughness height to the film thickness; this was extended to an annular channel with one wetted wall in reference 4. It was considered, however, that the roughness height data obtained for air–water systems could not justifiably be applied to the present steam–water tests. Only a qualitative comparison with the results of the previous theoretical treatments will therefore be given.

By adapting the theory developed by Hsu [7] for subcooled boiling Hewitt [3] was able to predict the heat flux required to cause the onset of bubble nucleation in annular climbing film flow. On plotting the heat flux for nucleation against quality, for a series of mass flow rates, it was found that approximately linear relationships were obtained; the computed nucleation heat flux increases with increasing mass flow rate and with increasing quality. The present data—see Fig. 7—show the same trends and are therefore in qualitative agreement with the theory. As was stated earlier, however, the results are somewhat erratic and fell in rather broad bands rather than on individual lines for each mass velocity; in this connection, however, it should be borne in mind that the theory assumes an idealized surface with a full range of active sites. The stainless steel heater used would almost certainly not fit this specification.

In reference 4, experiments are reported on the stability of the liquid films in air–water

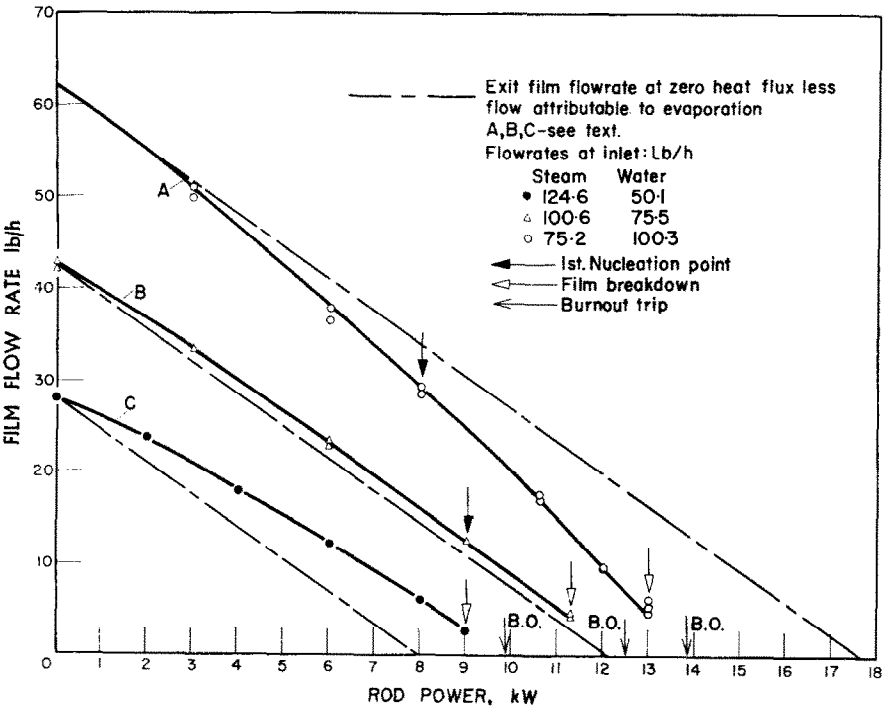

FIG. 10. Effect of power on the film flow rate at the end of the heated section. (Mass flow rate = $6{\cdot}4 \times 10^4$ lb/ft^{2}h)

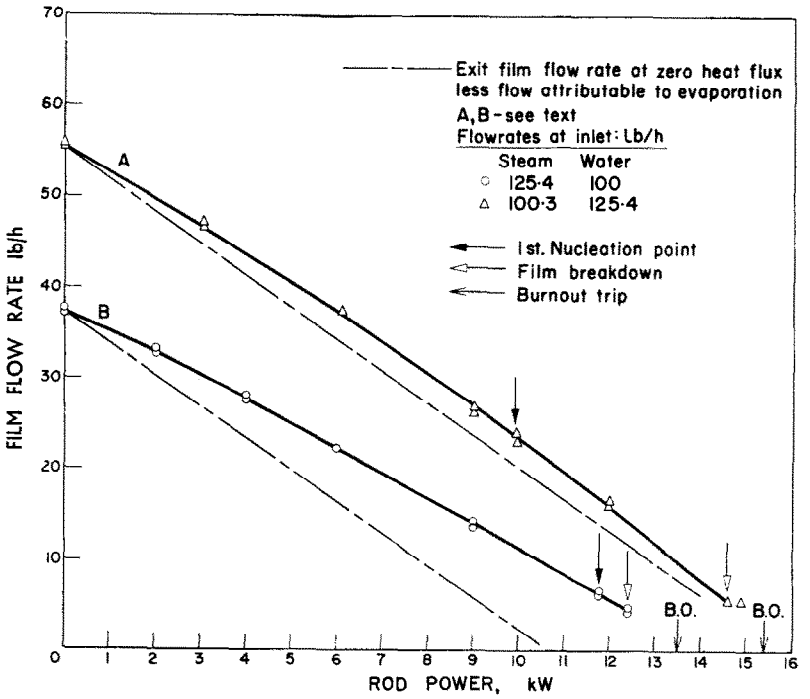

FIG. 11. Effect of power on the film flow rate at the end of the heated section. (Mass flow rate = $8{\cdot}3 \times 10^4$ lb/ft^{2}h)

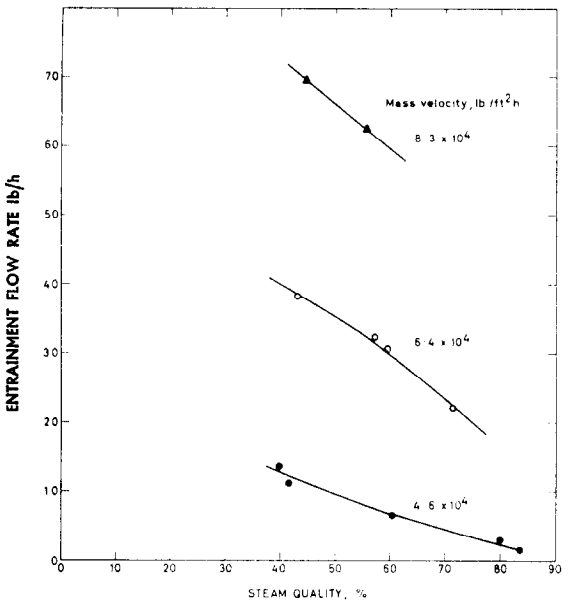

FIG. 12. Entrainment flow rate at the end of the heating section as a function of mass flow rate and quality. (Heat flux zero.)

annular flow. It was shown in these experiments that spontaneous breakdown of the liquid film did not occur. When a dry patch was formed artificially, the minimum liquid rate at which it was re-covered (the "minimum wetting rate") was found to decrease with increasing gas flow-rate. This latter observation was in accord with the theoretical predictions of Hartley and Murgatroyd [8]. The present results for film breakdown are plotted in Fig. 13; there is a great amount of scatter, but this is quite explicable if it is postulated that *all* the results shown are *below* the "minimum wetting rate" as defined above. The actual value observed for film flow rate at the breakdown point will then depend on what means is available to *initiate* the breakdown. This initiating mechanism could be the nucleation of a steam bubble, the dry area formed at the nucleation site becoming permanent. More than half the points shown in Fig. 13 (those denoted by +) have been obtained under conditions in which nucleation could be occurring in the region of the breakdown point (as deduced from Fig. 7). If the breakdown is not

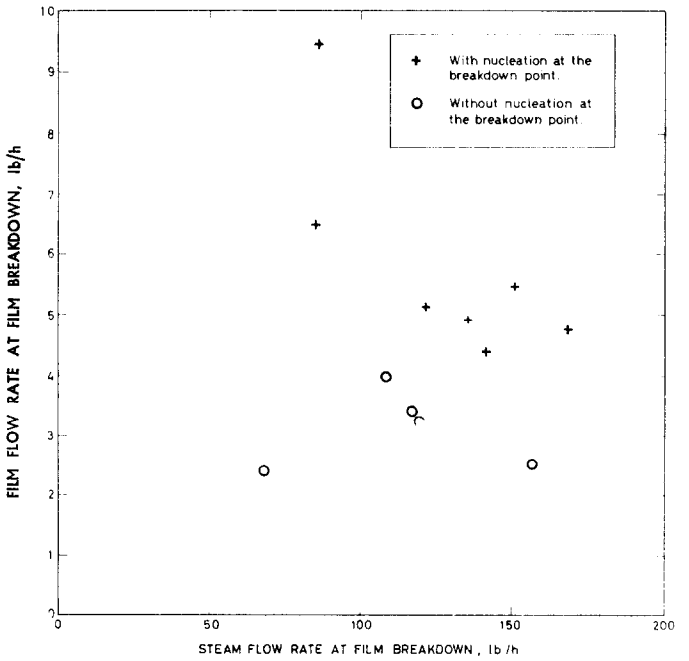

FIG. 13. Film flow rate at the initiation of film breakdown.

initiated by nucleation it could be caused by some small irregularity on the surface or by a slight maldistribution of flow causing drying out on one side of the rod. Figure 13 shows that, in the absence of nucleation, the film is stable to much lower values of flow rate (points denoted by ○).

Norman and McIntyre [9] have suggested that forces caused by difference in surface temperature are important in the breakdown of liquid films on surfaces; the temperature differences occur because of the wavy nature of the film and they lead to surface tension differentials which disrupt it. Norman and McIntyre, however, were working with films in contact with air, whereas in the present experiments the water film was in contact with steam at the saturation temperature. The surface is, therefore, probably very nearly isothermal and the effects described by these workers might not occur

The curves of film flow rate versus power presented in Figs. 9–11 contain important information of a new type and are worth close consideration. To assist in the discussion of these curves it will be helpful to consider a hypothetical example such as that illustrated in Fig. 14, where the local flow rate in the liquid film is plotted against position on the rod. For

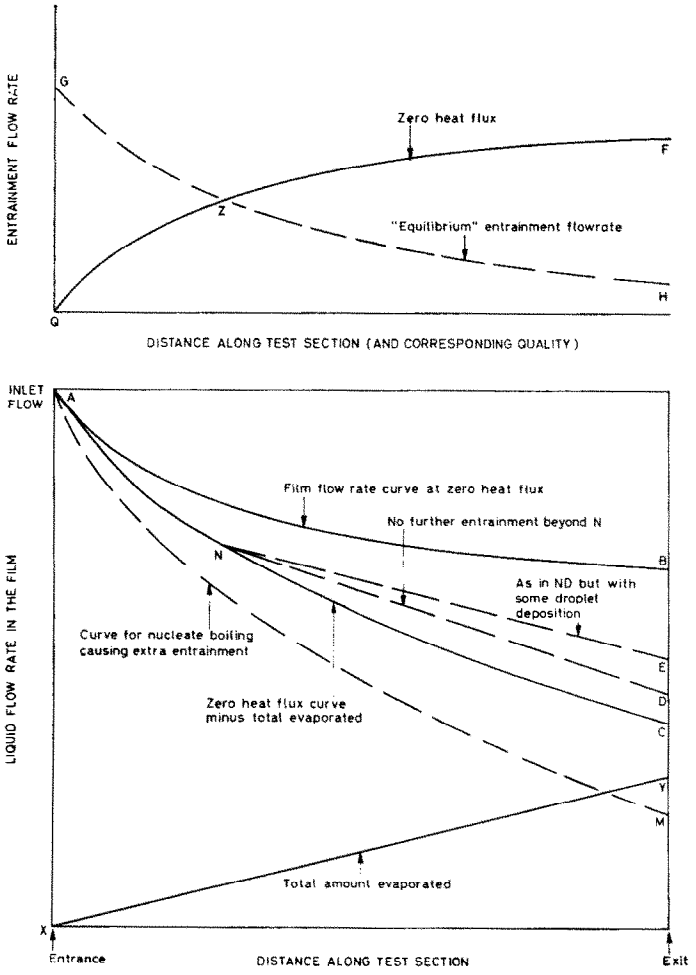

FIG. 14. Film flow rate as a function of heater length—(hypothetical).

zero heat flux, let us assume that a line AB is obtained (evidence for this shape is available in reference 11); suppose that a heat flux is applied causing evaporation, the total amount evaporated being shown as a function of length by the line XY. Assuming that no change occurs in the amount of entrained liquid, a line AC is obtained for film flow rate by subtracting XY from AB (AND). The quality, however, changes along the heater length (in a manner which can easily be computed), and as it does so, both the rate of entrainment and the *potential* total amount of entrainable liquid will be different. This latter is referred to as the "equilibrium" entrainment, and is the flow rate of entrained liquid which would be found in a non-evaporating (i.e. a constant quality) system in a very long tube. In the upper part of the figure the flow rate of entrained liquid is plotted (QF, i.e. AB inverted). As we shall see below, the equilibrium entrainment flow may either increase or decrease with increasing quality (at constant total mass flow). Figure 12, however, shows that all the present data are in a region in which the entrainment flow rate is lower the higher the quality; so in Fig. 14 an arbitrary curve, GH, is drawn, showing the equilibrium flow rate of entrained liquid corresponding to the local value of quality; i.e. although the abscissa is the position along the flow tube, the line GH is determined by the *quality* corresponding to each position. The shape of the film flow rate curve will, of course, be influenced all along the test section since the increase of gas velocity is certain to affect the *rate* of entrainment; to simplify this discussion, however, let us assume that the initial part of the curve is the same as in the zero heat flux case. The entrainment curve follows the line QF until it cuts the equilibrium line GH at Z. Beyond this point, no further entrainment action occurs and liquid is lost from the film solely by evaporation; the film flow rate curve is therefore AND. Deposition of the liquid which was entrained in the first part of the test section will possibly occur; this would lead to a further modification of the film flow rate curve giving ANE. The high-speed ciné films show clearly that bubble nucleation gives rise to extra entrainment; in cases where nucleation occurred, therefore, this could lead to a curve of film flow rate versus length such as line AM.

Figure 14 shows hypothetical plots of film flow rate against length; what was actually obtained in the present experiments was a plot of film flow rate at the *end* of the heater as a function of heat flux. The sort of curves one might expect from the factors discussed above and illustrated in Fig. 14 are shown in Fig. 15.

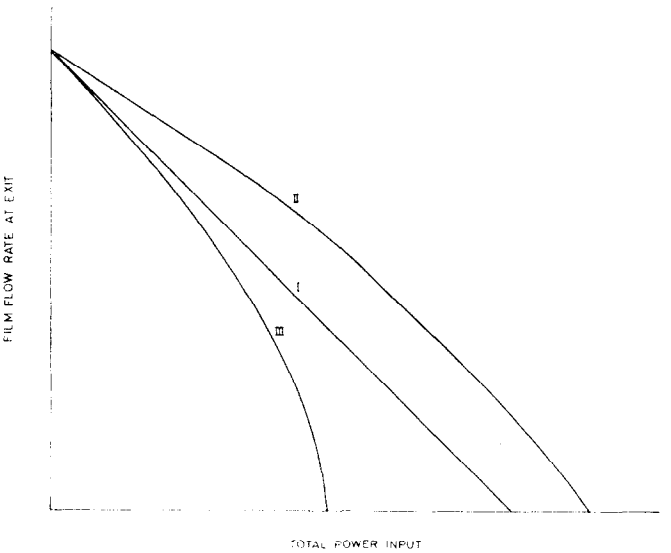

FIG. 15. Types of exit flow rate/power curves.

On curve I, the behaviour typified by line AC in Fig. 14 is occurring; the film flow rate at outlet is given by the value at zero heat flux minus the total evaporation. Curve II on Fig. 15 would occur if the entrainment had been suppressed and if deposition were occurring (see lines AND and ANE on Fig. 14) and curve III might be obtained when nucleation occurs (see line AM in Fig. 14).

Curves of type I are obtained only when the initial entrainment is in any case small (e.g. line C in Fig. 9). Curves of type II are seen in Figs. 10 (line B and C) and 11 (line A and B). Type III curves are obtained when the mass flow rate and/or quality is low (lines A and B in Fig. 9, and line A in Fig. 10). This is clearly the region in which nucleation is most likely to occur, but it should be noted that the curves begin to deviate from the "evaporation lines" well before the first nucleation site was observed. It may be, however, that some of the nucleation sites are active but have not been observed (this is not likely) or, alternatively, that jets of liquid are being ejected from the nucleation site into the steam core—a phenomenon which has been observed by Semaria [10]. This suggestion may explain the appearance of a "foggy" region near the surface of the heater which occurred on applying heat in the tests being discussed.

The broader result from the present experiments is the confirmation of the essentially integral nature of the burnout phenomenon. The burnout point appears to correspond quite closely with the point at which the liquid film has been lost by evaporation plus entrainment. It is not possible to separate the effects of suppression of entrainment from those of deposition in the present tests (see lines AND and ANE on Fig. 14), and it is not likely, with a heated section only $14\frac{1}{2}$ in long, that any sort of equilibrium condition will be reached.

5. DISCUSSION OF PREVIOUS WORK IN THE LIGHT OF THE PRESENT RESULTS

In the work described above, a short test section was used. It is of interest to consider what might happen in a long test section, where the rate of change of quality with length may be sufficiently low to allow the entrainment to approach equilibrium at every point. The effect of bubble nucleation on entrainment will, for the moment, be ignored.

A plot of equilibrium entrainment flow rate against quality, at constant mass flow rate, may be something like curve ABCD in Fig. 16. (As will be seen below, this shape of curve is suggested by previous air–water experiments). The total water rate is indicated by line ED and the difference between lines ED and ABCD is the film flow rate, line FD.

Consider now the behaviour of the system for an inlet quality x_i (Fig. 16). The flow is, by definition, at equilibrium so the film flow rate and entrainment at the inlet are given by the values on the ordinate corresponding to the points H and G where the line XY cuts the lines FD and ABCD respectively. As the flow proceeds along the channel, water is evaporated and the quality rises. In the range x_i to x_m, the entrainment increases (along line GC). If the system is maintained at equilibrium entrainment, deposition will occur as the quality rises from x_m up to 100 per cent along the channel. Burn out (defined as the point at which the film flow rate is zero) would therefore only occur at 100 per cent outlet quality. This is, of course, quite contrary to fact.

If it is assumed that the uptake of liquid into the gas core is rapid in the quality range x_i to x_m and that deposition is slow in the range $x > x_m$, then the entrainment flow might follow a line such as GCJ′ (Fig. 16). This line meets the line of total water flow (ED) at J′ corresponding to quality x'; this means that the liquid film flow is zero and, hence, burnout occurs at this quality. As the length increases, however, there is more time for deposition and the entrainment flow curve might shift to CJ″ and further to CJ‴ with corresponding qualities at burnout of x'' and x'''.

The total power (ψ_{Bo} Btu/h say) given to the fluid to attain burnout is related to the inlet and outlet qualities:

$$\psi_{Bo} = GHA(x_{Bo} - x_i) \qquad (2)$$

where x_{Bo} is the outlet quality at burnout, G the mass velocity (lb/ft² h, say), H the latent heat (Btu/lb) and A the channel cross-sectional area (ft²). The arguments outlined above and illustrated in Fig. 16 would indicate that ψ_{Bo}

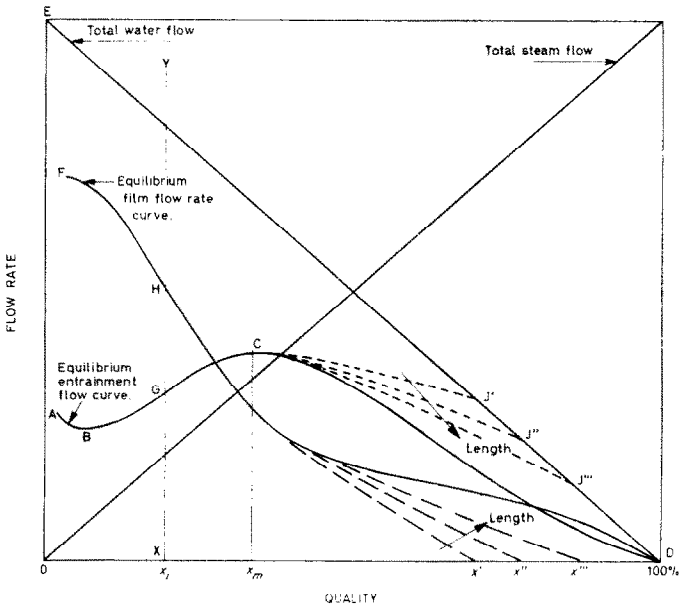

FIG. 16. Hypothetical film flow rate and entrainment rate plots at constant mass flow rate.

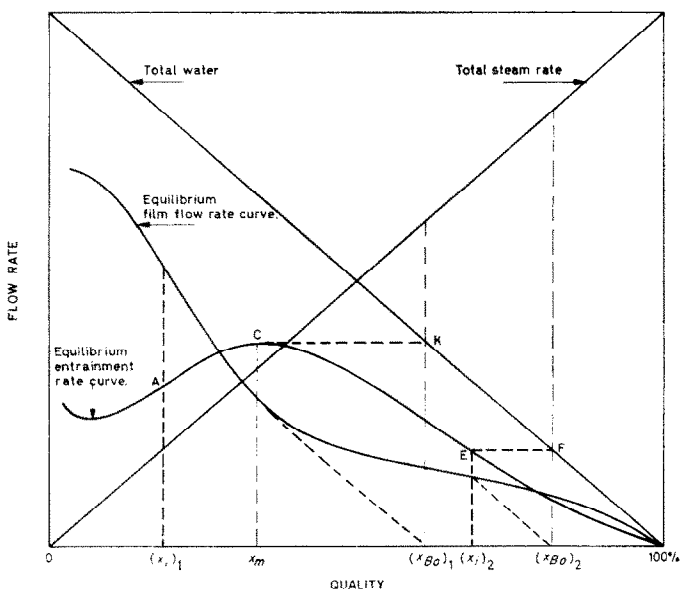

FIG. 17. Explanation of burnout with no deposition.

should increase with increasing length. Results obtained at Harwell [14] for high pressure steam water flow in internally heated annuli with length to equivalent diameter ratio (L/D) in the range 14–115, and also recent work at CISE (Italy) [13] for round tubes with $L/D < 150$, seem to confirm this trend. However, the CISE workers have found [13] that for $L/D > 150$, the total power (ψ_{Bo}) is constant and does not change with increasing length. This is difficult to explain on the above argument about deposition.

above to explain the constancy of burnout power, ψ_{Bo}, for $L/D > 150$ must be reconciled with the fact that ψ_{Bo} decreases with decreasing L/D for $L/D < 150$. The assumption has been made that if the entrainment is less than that given by lines such as ABCD in Fig. 16, then it rapidly rises to this value. This assumption cannot be valid for short channels and the result obtained for these channels will be highly dependent on the mode of mixing of the phases at the inlet. It is believed from air–water tests [15], however,

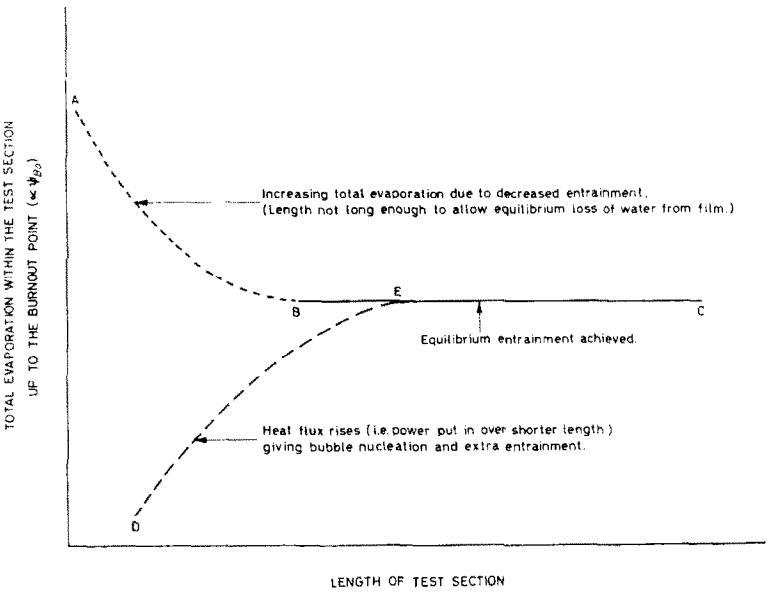

FIG. 18. Postulated curves for the effect of length of test section on the total amount of liquid evaporated up to the burnout point. (Fixed inlet quality and mass flow rate.)

One possibility is that redeposition is negligible and that practically all the entrained liquid remains in the steam phase. The entrainment flow rate versus quality curves would thus be like ACK and EF in Fig. 17 for inlet qualities $(x_i)_1$ and $(x_i)_2$, below and above x_m respectively. One interesting consequence of the type of behaviour shown in Fig. 17 is that for inlet qualities below x_m, the quality at outlet at burnout is independent of the inlet quality. Hence, a plot of ψ_{Bo} against x_{Bo} for $x_i < x_m$ would be a vertical line, the burnout power increasing with increasing inlet quality [see equation (2)]. This sort of result is, in fact, obtained [12].

The postulate of negligible deposition invoked

that the type of mixing used in the Harwell tests [14, 12] would give an inlet film flow rate which was *greater* than the equilibrium. It would be expected, therefore, that the burnout power (ψ_{Bo}) would increase with decreasing length (as in line AB in Fig. 18). As was stated above, however, the opposite effect is found.

Though the *total power* for burnout decreases with decreasing length for $L/D < 150$, the *heat flux* increases. This increase in heat flux would give rise to an intensification of the nucleation of steam bubbles and, as we have seen, this would cause extra entrainment. This would probably override the entrainment disequilibrium effect (line AB, Fig. 18) and give rise to the observed

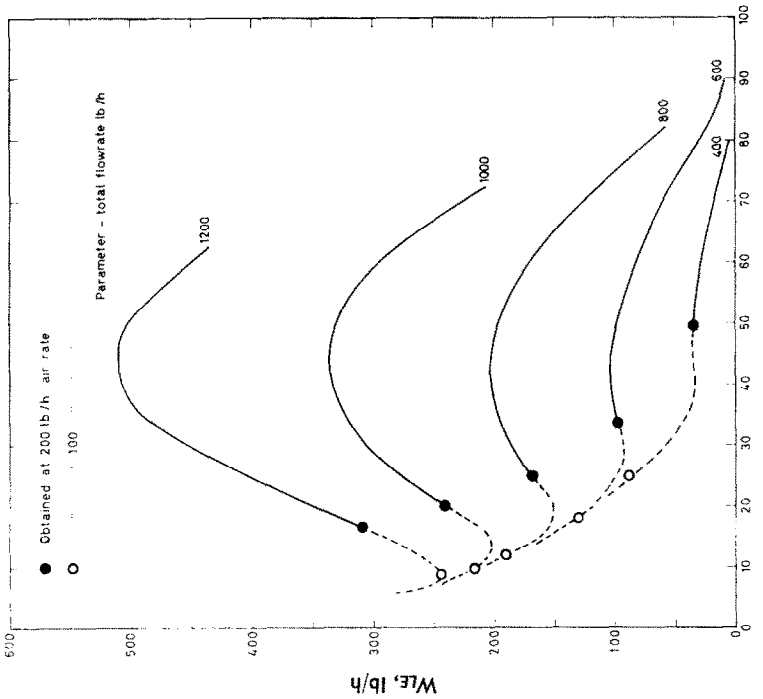

FIG. 20. Air–water entrainment flow rate results plotted as a function of "quality".

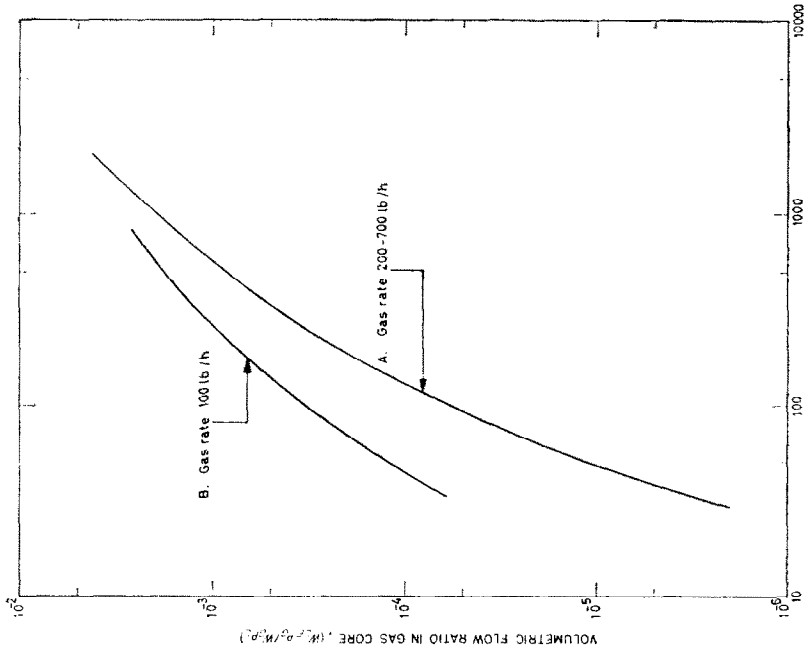

FIG. 19. Air–water entrainment results.

effect (line DE). The fact that the total power does not vary with length for $L/D > 150$ does not mean that no nucleation is occurring, but merely that nucleation is no longer causing significant entrainment. Nucleation may not be as effective in entraining at higher pressures because of the much smaller bubble size.

Although the above arguments are largely conjectural, it is worthwhile to take a further step and to predict the form of the burnout power curves from previous Harwell air–water results for entrainment. The following assumptions are made (most of them follow directly from the argument given above):

(i) Burnout occurs when the liquid film is completely removed by evaporation and entrainment.

(ii) The imaginary tube is long and the rate of evaporation low.

(iii) If the equilibrium entrainment flow rate increases with increasing quality then at all points the equilibrium rate is obtained, which is assumed to be as given in Fig. 16. (This is one of the reasons for assuming the tube to be long.)

(iv) No deposition of the entrained phase takes place. The consequence of this assumption is that if the equilibrium *isothermal* entrainment flow rate is smaller at higher qualities (as in Fig. 12), then the entrainment will remain at the highest value it has reached within the test section.

(v) Nucleation has no effect on the entrainment. (If a long tube is used then the heat flux is low and the intensity of nucleation is small.)

(vi) The evaporation process along the tube is equivalent to the gain of one pound of air for the loss of one pound of water.

In previous reports [6, 11], a study of entrainment in air–water flow in a long vertical 1¼ in bore tube is described. In the second of these reports [6], measurements of the diametrical distribution of entrainment flow are described for a series of air and water flow rates. These distributions were obtained at a point far from the liquid injector and may be approaching the equilibrium condition. Integration across the diameter of the tube led to an evaluation of the total entrainment flow (W_{LE}). It was found that W_{LE} was correlated for air rates in the range 700–200 lb/h by plotting the volumetric flow ratio, $W_{LE}\rho_G/W_G\rho_L$ against W_L where W_G is the gas rate, W_L the total liquid rate and ρ_G and ρ_L the gas and liquid densities respectively. The results fell on a single line, line A in Fig. 19. At the lowest gas rate used (100 lb/h) the entrainment was higher and the results fell on line B.

Taking constant total air/water flow rates of 1200, 1000, 800, 600 and 400 lb/h, the entrainment was calculated as a function of "quality" (ratio of air mass flow to total mass flow), and the results are plotted in Fig. 20. The range between 100 and 200 lb/h of air flow has been interpolated and the region below 100 lb/h air extrapolated freely as indicated by the dotted lines. The entrainment flow rate increases with increasing mass flow rate and passes through a maximum with increasing quality. There is also a suggestion of a minimum in the curves at low quality. Using the results in Fig. 20 and making the assumptions listed above, "burnout curves" were calculated and are shown in Figs. 21 and 22 plotted against outlet and inlet quality respectively. The curves are plotted as "total evaporation" rather than as power or heat flux. The assumptions made in the analysis imply that the burnout *heat flux* will be inversely proportional to the length of the test section.

The form of the curves shown in Fig. 21 is very similar to those actually obtained at high pressure [12]. The vertical drop in burnout heat flux at constant exit quality which occurs in part of all the curves, arises because of the maxima in the entrainment curves in Fig. 20 (see Fig. 17 and the associated text).

If the inlet quality is greater than that for maximum entrainment, the burnout curve shows a negative slope. The relative position of the "tail" of the predicted "burnout" curves is similar to that observed previously in burnout work [12]. At low mass velocities, the increase of entrainment with decreasing quality at low qualities is sufficient to bend the burnout curves over (Fig. 18). Again this is fully in accord with the observed data [12]. Since the minimum in the entrainment curve with decreasing quality corresponds with the approach to "churn flow",

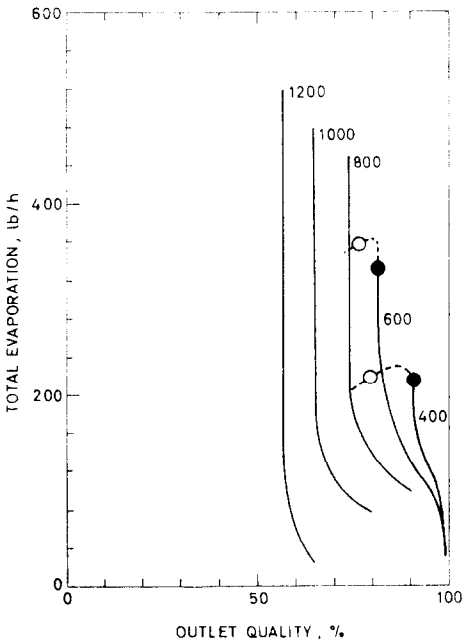

FIG. 21. Burnout curves calculated from air–water data.
○ Corresponding to 100 lb/h air
● Corresponding to 200 lb/h air
Parameter—total flow rate lb/h.

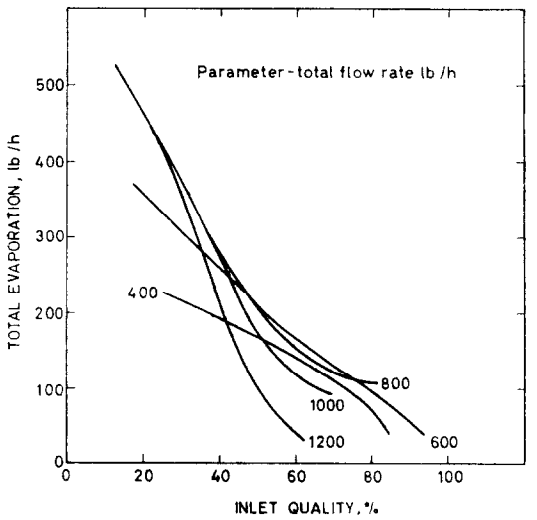

FIG. 22. Burnout curves calculated from air–water data based on inlet quality.

suppression of oscillations in the system in this region may have a profound effect.

5. CONCLUSION

The experiments described in this report have allowed direct observation of the burnout phenomenon in annular flow. The measurements of film flowrate have shown that the burnout corresponds quite closely with the point at which the film flow rate becomes zero; the onset of film breakdown occurs at a small, but finite, value of the film thickness. These film flow rate determinations have also allowed several important inferences to be made about the processes governing entrainment.

The broad conclusion from the experimental results and discussion presented here is that burnout is an essentially integral phenomenon; the more liquid entrained along the flow channel, the lower the total evaporation, and the lower the burnout heat flux. Entrainment occurs either by the normal two phase mechanism of wave entrainment or is caused by the throwing out of liquid when a bubble is nucleated within the film. It cannot be decided from the present results whether or not re-deposition at the end of the channel, of material entrained at the beginning, is an important mechanisms. Ignoring the effects of deposition in predicting burnout curves from the air–water data, however, gave results which were suggestively like the burnout curves found in practice.

The experiments described above were necessarily preliminary but they have pointed the way to further work which can be done using similar principles and techniques.

ACKNOWLEDGEMENTS

The authors wish to acknowledge the assistance of A.E.R.E. Photographic Section and the help of L. E. Gill with computations.

REFERENCES

1. G. BIDDLE, A. DOWNS and G. W. PEAGRAM, A burnout detector. *AERE-M* 1160 (1962).
2. J. G. COLLIER, Burnout in liquid cooled reactors, *Nuclear Power* **6**, 61, June issue (1961); **6**, 63, July issue (1961).
3. G. F. HEWITT, Some calculations on holdup, heat transfer and nucleation for steam water flow in a 0·5 cm bore tube. *AERE-R* 3984. H.M. Stationery Office, London (1962).

4. G. F. HEWITT and P. M. C. LACEY, The breakdown of the liquid film in annular two-phase flow, *Int. J. Heat Mass Transfer* **8**, 781 (1965). [Also *AERE-R* 4303 (1963).]
5. G. F. HEWITT, Interpretation of pressure drop data from annular channels. *AERE-R* 4340. H.M. Stationery Office, London (1963).
6. L. E. GILL, G. F. HEWITT and P. M. C. LACEY, Sampling probe studies of the gas core in annular two-phase flow. Part II: Studies of the effect of phase flow rates on phase and velocity distribution, *Chem. Engng Sci.* **19**, 665 (1964). [Also *AERE-R* 3955 (1963)].
7. Y. Y. HSU, On the size range of active nucleation cavities on a heating surface. Paper no. 61-*WA*-177 presented at the Winter Annual Meeting, ASME, New York (1961).
8. D. E. HARTLEY and W. MURGATROYD, Criteria for the break-up of thin liquid layers flowing isothermally over solid surfaces, *Int. J. Heat Mass Transfer* **7**, 1003 (1964). (Also Nucl. Res. Memo. *Q*5, Queen Mary College, London, 1961.)
9. W. S. NORMAN and V. MCINTYRE, Heat transfer to a liquid film on a vertical surface, *Trans. Inst. Chem. Engrs* **38**, 301 (1960).
10. R. SEMARIA, La Strioscopie appliquée a l'étude de l'ebullition et du dégazage, To be published in *La Houille Blanche*.
11. L. E. GILL, G. F. HEWITT, J. W. HITCHON and P. M. C. LACEY, Sampling probe studies of the gas core in annular two-phase flow. Part I: The effect of length on phase and velocity distribution, *Chem. Engng Sci.* **18**, 525 (1963). [Also *AERE-R* 3954 (1962).]
12. A. W. BENNETT, J. G. COLLIER and P. M. C. LACEY, Heat transfer to mixtures of high pressure steam and water in an annulus. Part II: The effect of steam quality and mass velocity on the "burnout" heat flux for an internally heated unit at 1000 psia. *AERE-R* 3804 (1961).
13. C. LOMBARDI, CISE, Milan; private communication (July 1963).
14. A. W. BENNETT and H. A. KEARSEY, Heat transfer to mixtures of high pressure steam and water in an annulus: Part IV: The effect on burnout of length and diameter of the heater. *AERE-R* 3961 (To be published).
15. G. F. HEWITT and A. T. G. STEVENS, Two-phase annular flow of air–water mixtures in an annulus, Part II: Measurement of liquid film flow rates and of the effect of length. *AERE-R* 4302 (To be published).

Résumé—On a étudié le comportement d'un film d'eau sur la partie centrale chauffée d'une portion de tube annulaire dans laquelle s'écoule de la vapeur d'eau à pression atmosphérique, l'eau ayant été introduite à travers une paroi poreuse. La paroi extérieure en verre du tube annulaire était chauffée pour éviter la condensation et le dépôt de gouttelettes et ainsi la surface de la partie centrale était rendue visible clairement. Le début de la nucléation dans le film a été mis en évidence et les conditions pour son déclenchement ont été déterminées et comparées avec les prévisions théoriques; dans d'autres expériences de caléfaction, on a fait des mesures de flux de chaleur et on les a reliées à l'écoulement du film résiduel mesuré sur la partie centrale chauffée. Des études visuelles et photographiques ont révélé une condition relativement stable de la rupture du film ascendant, avec des ruissellments autour des endroits secs, avant que la caléfaction totale se produise.

La vitesse d'écoulement du film résiduel à laquelle des taches sèches apparaissaient était en effet très faible et le phénomène de caléfaction était clairement le simple résultat de la perte totale d'eau du film par évaporation et entraînement; la valeur locale du flux de chaleur à l'endroit de la caléfaction était évidemment seulement d'importance secondaire. Il était évident que la germination de bulles dans le film pourrait contribuer d'une façon appréciable à la perte par entraînement à des flux de chaleur élevés.

Zusammenfassung—Über das Verhalten eines Wasserfilms an dem beheizten zentralen Stab einer Messstrecke ringförmigen Querschnitts, in der Dampf bei Atmosphärendruck strömt und das Wasser durch eine poröse Wand zugeführt wird, wurden Untersuchungen angestellt. Die äussere Glaswand des Ringrohres wurde beheizt, um Kondensation und Tropfenbildung zu verhindern. So blieb die innere Staboberfläche deutlich sichtbar. Der Beginn der Keimbildung innerhalb des Films wurde gezeigt und die Bedingungen für ihr Entstehen festgelegt und mit theoretischen Vorhersagen verglichen. In anderen Versuchen wurden "burnout" oder "dry-out" Wärmestromdichten gemessen und mit der gemessenen restlichen Filmströmung an dem beheizten Stab in Beziehung gesetzt. Visuelle und photographische Studien ergaben eine relativ stabile Bedingung für das Auflösen des hochsteigenden Filmes und zeigten kleine Ströme um die ausgetrockneten Stellen ehe der Burnoutdetektor ansprach. Die Geschwindigkeit der restlichen Filmströmung, bei der trockene Stellen auftraten, war tatsächlich sehr gering und das "burnout" Phänomen war klar ersichtlich ganz einfach das Ergebnis eines totalen Wassermangels am Film durch Verdampfung und Abführung; die lokalen Werte der Wärmestromdichte an der Burnoutstelle hatten eindeutig zweitrangige Bedeutung. Es ergab sich klar, dass die Blasenbildung im Film merkbar zu diesem Mangel durch Abführen von Dampf bei hohen Wärmestromdichten beitrug.

Аннотация—Проведены исследования поведения водяной пленки на нагретом центральном стержне кольцевого рабочего участка, в котором находился движущийся пар при атмосферном давлении, а вода подавалась через проистую стенку. Наружная стеклянная стенка кольцевого канала нагревалась, чтобы не происходила конденсация пара и оседание капель и можно было наблюдать за поверхностью стержня. Наблюдалось начало образования пузырьков внутри пленки и определяись условия их возникновения, которые сравнивались с теоретическими. В других экспериментах по «высыханию» проводились измерения теплового потока, которые сопоставлялись со случаем остаточного пленочного течения на нагретом стержне.

Визуальные и фотографические исследования показали относительно стабильное условие нарушения наползающей пленки (с ручейками вокруг высохших чуастков) перед началом работы механизма высыхания.

Скорость течения остаточной пленки, при которой появлялись сухие участки, была в действительности очень небольшой и было ясно, что явление «высыхания» происходило просто в результате полной потери воды пленкой за счёт испарения и уноса; локальное значение величины потока тепла в месте высыхания, очевидно, играло вторичную роль. Было очевидно, что пузырьковые ядра в пленке могли значительно влиять на нотерю уносом при больших значениях потока тепла.